

A reflectance band ratio used to estimate suspended matter concentrations in sediment-dominated coastal waters

D. DOXARAN*, J.-M. FROIDEFOND and P. CASTAING

Université Bordeaux I, Département de Géologie et Océanographie, UMR 5805 EPOC, Avenue des Facultés, 33405 Talence cedex, France

(Received 29 November 2001; in final form 6 June 2002)

Abstract. This letter presents an empirical relationship that may be used to estimate the suspended particulate matter concentrations in highly turbid waters from remote sensing reflectance measurements. Numerous measurements carried out in the Gironde estuarine waters (France) in 2000 and 2001 are presented and analysed. It was observed that the near-infrared (850 nm) reflectance was weakly correlated with the total suspended matter concentration (TSM_c) measured in surface waters. A strong correlation ($r=0.91$) was obtained between the ratio of the near-infrared and visible (550 nm) reflectance and TSM_c , which could provide an accurate calibration curve for data from Système Probatoire de l'Observation de la Terre (SPOT), Landsat and Indian Remote Sensing (IRS) satellite sensors. The reflectance ratio reduced the effects of changes in illumination conditions and sediment type (grain-size, refractive index). The calibration function obtained, successfully applied to the Gironde, should be applied in other sediment-dominated coastal waters.

1. Introduction

One of the applications of visible and near-infrared remote sensing in oceanography is to relate the measured water-leaving signal to the constituents of the waterbody (e.g. phytoplankton, dissolved organic matter, mineral particles). With remotely sensed imagery, the process generally includes a preliminary correction for atmospheric effects. Then, theoretical or empirical algorithms may be used to derive information about water constituents (optical properties, concentrations) from the estimated water-leaving signal. Considering sediment-dominated coastal waters, refined algorithms are needed to estimate accurately the suspended particulate concentrations from ocean colour remotely sensed data (e.g. Bowers *et al.* 1998, Robinson *et al.* 1998, Froidefond *et al.* 1999, Moore *et al.* 1999) notably to provide calibration data for numerical hydro-sedimentary models (Siegle *et al.* 1999). The objective in this study is to develop such an inversion algorithm, which could permit the accurate estimation of the total suspended matter concentration (TSM_c) distributions from remotely sensed data, independently of the date of acquisition. The aim is to provide a calibration function relating reflectance to TSM_c in spectral bands of actual and future fine spatial resolution satellite sensors.

* Corresponding author: e-mail: d.doxaran@epoc.u-bordeaux.fr

2. Theory

The remote sensing reflectance signal (R_{rs} in sr^{-1}) is defined by (Mobley 1994)

$$R_{rs} = \frac{L_w}{E_d} \quad (1)$$

where L_w (in $\text{W m}^{-2} \text{sr}^{-1} \text{nm}^{-1}$) is the water-leaving radiance and E_d (in $\text{W m}^{-2} \text{nm}^{-1}$) is the downwelling irradiance.

According to Morel and Gentili (1996), the above water R_{rs} signal can be expressed as a function of the irradiance reflectance (R , unitless) at null depth, noted 0^- ($R = [E_u(0^-)/E_d(0^-)]$, with E_u the upwelling irradiance)

$$R_{rs} = \frac{0.529}{(1 - \bar{r}R)} \frac{R}{Q} \quad (2)$$

where the term 0.529 results of the air–water Fresnel reflection and refraction effects for the remote sensing configuration, \bar{r} is the water–air reflection and is of the order of 0.48, Q is the upwelling irradiance to upwelling radiance ratio [$E_u(0^-)/L_u(0^-)$] (in sr) which would be π if the L_u distribution were isotropic, but may vary between approximately 3.1 and 5.6.

The irradiance reflectance is written as a function of the inherent optical properties (IOPs) of the waterbody, namely the absorption and backscattering coefficients a and b_b (in m^{-1}), according to (Gordon *et al.* 1975)

$$R = f' \frac{b_b}{a + b_b} \quad (3)$$

where the value of f' is 0.324 for a Sun close to the zenith (Morel and Gentili 1996). Thus, the remote sensing reflectance is finally written

$$R_{rs} = 0.529 \frac{a + b_b}{a + (1 - \bar{r}f')b_b} \frac{f'}{Q} \frac{b_b}{a + b_b} = 0.529 \frac{f'}{Q} \frac{b_b}{a + (1 - \bar{r}f')b_b} \quad (4)$$

which indicates its dependence on the IOPs and, according to Morel and Gentili (1993), on the illumination conditions and viewing directions through the f' and Q parameters.

3. Field measurements

Data were collected in the Gironde estuary during two successive summers (July and September 2000; July, August and September 2001) at four fixed stations located in the border of the main navigation channel, at the following distances from Bordeaux: 30, 52, 67 and 85 km (figure 1).

Optical data were recorded with a Spectron SE-590 spectroradiometer with 256 sensors in the interval 400–1100 nm (band width: 2.8 nm per sensor), following the measurement procedure described by Doxaran *et al.* (2002). The radiometer was directed vertically toward the water, 1 m above the surface, when measuring the upwelling radiance L_u , vertically directed toward a spectralon target when measuring the downwelling radiance L_d and directed toward the zenith when measuring the sky radiance L_s . The target is near Lambertian for solar zenith angles between 0–40°, as its reflectance (R_p) varies by only 3% (Dilligeard 1997). In these conditions, the downwelling irradiance E_d was ($\pi L_d/R_p$). Upwelling radiance measurements were

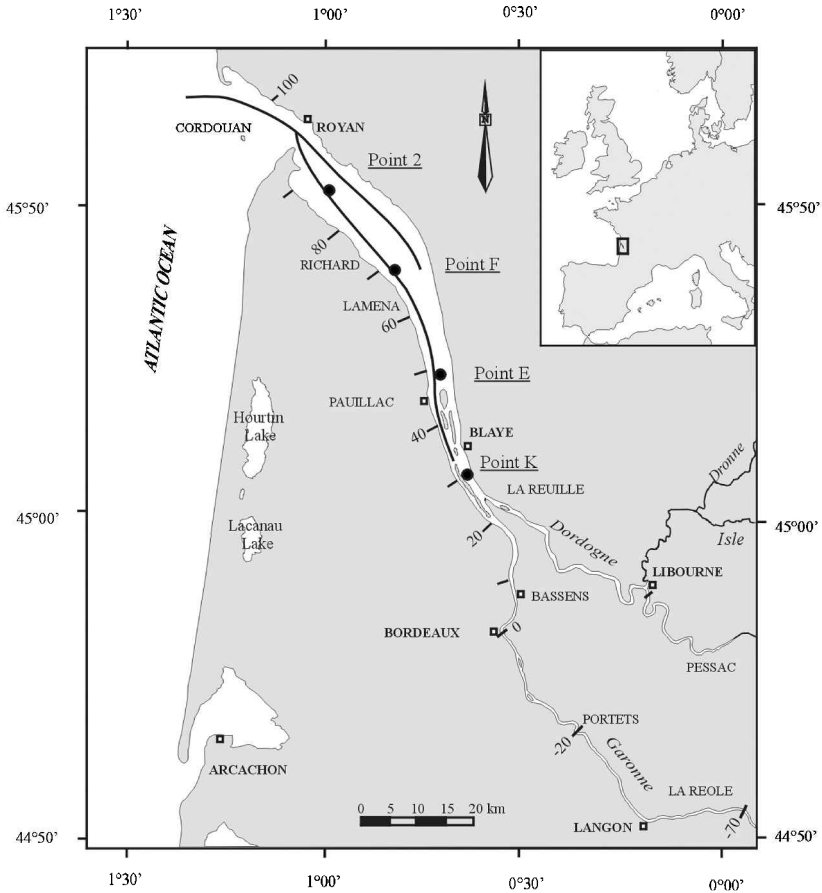


Figure 1. The Gironde estuary, located in south-west France. The lines represent the main navigation channels. Black circles locate the four fixed stations of field measurements.

corrected for skylight reflection effects (sky glint) by subtracting 2% of the measured sky radiance (Austin 1974), in order to estimate the water-leaving radiance (Mobley 1999). The measured remote sensing reflectance was finally given by

$$R_{rs} = R_p \frac{L_u - 0.02 L_s}{\pi L^d} \quad (5)$$

For each optical measurement, the TSM_c was measured near the surface (50 cm depth) by filtering a water sample on Whatman GF/F glass-fibre filters (diameter 47 mm, pore size 0.44 μm).

Field measurements were carried out when there was a clear blue sky (no cloud) and a quasi-plane water surface (wind speed close to 0 m s^{-1}). A total of 34 coincident R_{rs} and TSM_c [in the range (0.013–0.985 g l^{-1})] data samples, recorded in July 2000 (18 and 21 July 2000, four samples), September 2000 (25–29 September 2000, 22 samples), July 2001 (4 July 2001, one sample), August 2001 (25 August 2001, two samples) and September 2001 (10–13 September 2001, five samples), were available.

The measured R_{rs} typically increased with TSM_c in the range 400–1000 nm, notably at 550 and 850 nm which are the central wavelengths of Système Probatoire

de l'Observation de la Terre–High Resolution Visible (SPOT-HRV) and Landsat-Advanced Thematic Mapper (ETM)+ yellow-green and near-infrared spectral bands, respectively (figure 2). The largest increase was observed in the near-infrared wavelengths (700–900 nm) where R_{rs} was practically zero for a low $TSMc$ (0.013 g l^{-1}) and was about 0.1 sr^{-1} for a high $TSMc$ (0.985 g l^{-1}).

4. Results and discussion

Variations of the R_{rs} signal measured at 550 nm and 850 nm, denoted $R_{rs}(550)$ and $R_{rs}(850)$, were observed as a function of $TSMc$. As expected, $R_{rs}(850)$ increased with increasing $TSMc$ in the range 0.010 – 0.250 g l^{-1} ($r=0.79$) (figure 3). Over 0.25 g l^{-1} , $R_{rs}(850)$ tended to saturate. Concerning the visible wavelength, no significant correlation was found between $R_{rs}(550)$ and $TSMc$ (results are not presented here), which could lead to the following conclusion: reflectance measurements in visible and near-infrared bands do not allow an accurate estimation of $TSMc$.

It was observed that the reflectance ratio [$R_{rs}(850)/R_{rs}(550)$] was strongly correlated to $TSMc$ ($r=0.91$) (figure 4). Values were close to zero for the lowest $TSMc$ ($<0.050 \text{ g l}^{-1}$) as $R_{rs}(850)$ was close to zero, then rose to 110% for the highest $TSMc$. The error associated with each R_{rs} measurement depends on the residual error committed when correcting the measured L_u signals for skylight reflection effects. This residual error cannot be assessed from the data. However, it was observed that if a $\pm 7\%$ uncertainty is assumed for the [$R_{rs}(850)/R_{rs}(550)$] ratio, the polynomial function plotted on the graph ($R^2=0.97$) includes all data collected in 2000 and 2001. This function allows an accurate estimation of $TSMc$ from R_{rs} measurements.

To explain the obtained results, refer to equation (4) which indicates that R_{rs} is a function of both geometrical parameters, namely f' and Q , and of the IOPs, namely a and b .

The measurements were carried out for different tidal conditions (neap/spring tides) independently of the tidal cycle (ebb/flood tides, low/high water periods) and at different locations in the estuary. Consequently, they probably correspond to a variety of sediment grain-size and refractive index. Results of computations with an

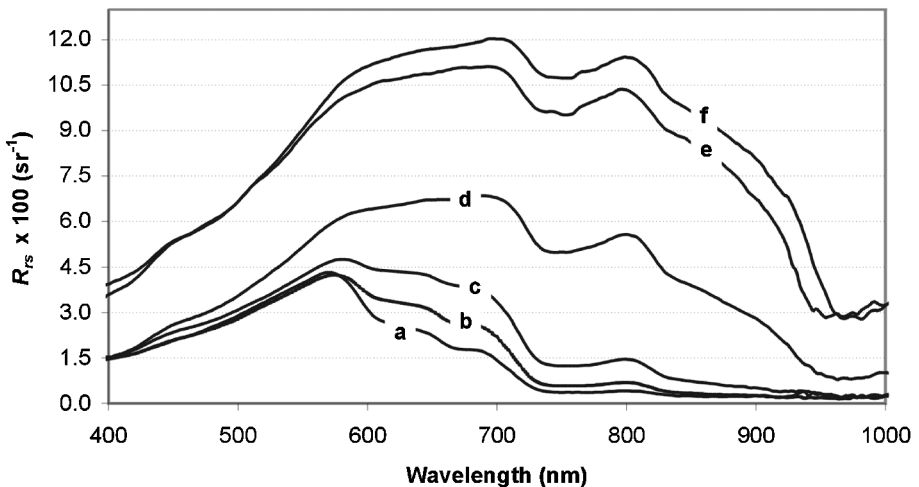


Figure 2. Examples of measured R_{rs} spectra for different $TSMc$: a, 0.013 g l^{-1} ; b, 0.023 g l^{-1} ; c, 0.062 g l^{-1} ; d, 0.355 g l^{-1} ; e, 0.651 g l^{-1} ; and f, 0.985 g l^{-1} .

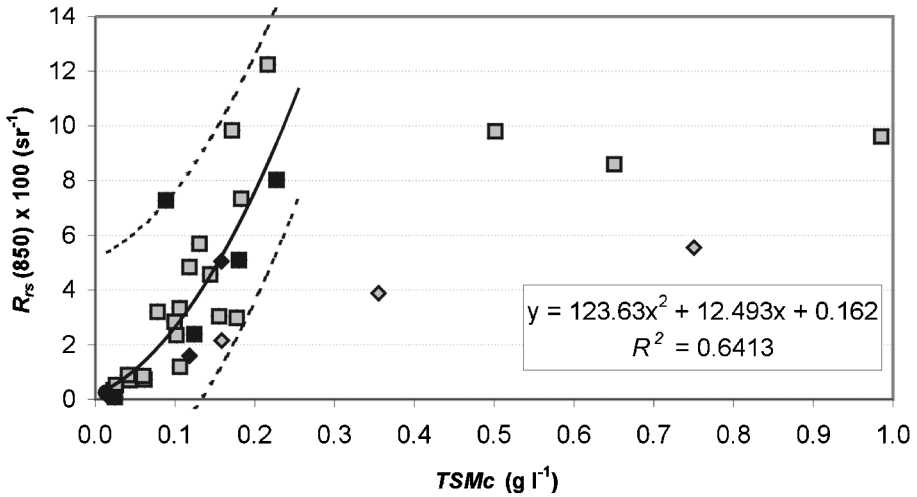


Figure 3. R_{rs} measured at 850 nm plotted against $TSMc$. Date of measurements: July (rhombus), August (circles) and September (squares) 2000 (grey points) and 2001 (black points). Plot of the second order polynomial regression. Plot of the function uncertainty including points in the range $0.01\text{--}0.25\text{ g l}^{-1}$.

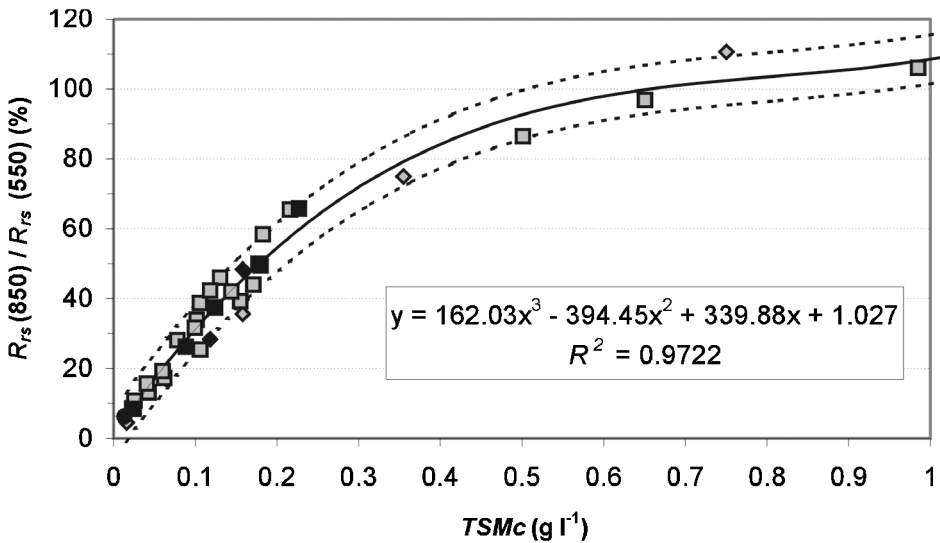


Figure 4. Ratio of reflectance [$R_{rs}(850\text{ nm})/R_{rs}(550\text{ nm})$] plotted against $TSMc$. Date of measurements: July (rhombus), August (circles) and September (squares) 2000 (grey points) and 2001 (black points). Plot of the third order polynomial regression and the $\pm 7\%$ reflectance ratio uncertainty which includes all points in the range $0.010\text{--}1.000\text{ g l}^{-1}$.

IOP model (Lahet 1999) have shown that the backscattering coefficient by sediment is highly dependent on the sediment type (grain-size, refractive index). Doxaran *et al.* (2002) have integrated these results into a reflectance model adapted to the Gironde estuary and observed that these variations of sediment type highly influence the

R_{rs} (850) signal, independently of the sediment concentration. Moreover, as illustrated by Morel and Gentili (1996), the f'/Q ratio depends on the illumination conditions (i.e. the solar zenith angle). As a conclusion, a part of the variations of the measured R_{rs} (850) signal (figure 3) was probably due to sediment type and solar zenith angle variations which occurred during the field campaigns.

According to equation (4), a ratio of the near-infrared (λ_1) and visible (λ_2) remote sensing reflectance can be approximately written

$$R_{rs}(\lambda_1)/R_{rs}(\lambda_2) = \left[\frac{f'}{Q}(\lambda_1) / \frac{f'}{Q}(\lambda_2) \right] \left\{ \frac{bb(\lambda_1) a(\lambda_2) + (1 - \bar{r}f'(\lambda_2))bb(\lambda_2)}{bb(\lambda_2) a(\lambda_1) + (1 - \bar{r}f'(\lambda_1))bb(\lambda_1)} \right\} \quad (6)$$

Doxaran *et al.* (2002) showed that the ratio within braces [equation (6)]: weakly depends on sediment type variations which induce variations of the bb coefficient; and is highly correlated with $TSMc$. Morel and Gentili (1993, 1996) showed that, for unvarying optical properties of a given waterbody, spectral variations of the f'/Q ratio are low, which could lead to a simplification of equation (6): $[(f'/Q)(\lambda_1)/(f'/Q)(\lambda_2)] \approx 1$. No measurements of the f' and Q were carried out during the field campaigns, but the relationships obtained tend to confirm this assumption. In fact, the $[R_{rs}(850)/R_{rs}(550)]$ reflectance ratio was highly correlated to $TSMc$, and depends weakly on illumination conditions and sediment type variations which occurred during the field measurements (figure 4). The relationship obtained plotted on the graph (figure 4) will permit the development of an invariant algorithm used to estimate the $TSMc$ in the Gironde estuary from remotely sensed data.

5. Conclusion

From numerous field reflectance measurements, an empirical relationship was established which allows the accurate estimation of suspended particulate matter concentrations in the Gironde estuary. This relationship is based on a simple reflectance ratio between near-infrared (850 nm) and visible (550 nm) wavelengths. While reflectance in the near-infrared allowed only an approximate estimation of $TSMc$ between 0.015–0.250 $g\ l^{-1}$, a high correlation coefficient ($r = 0.91$) was obtained between this ratio and $TSMc$, including all measurements collected during two successive low river flow periods on 2000 and 2001 and providing an accurate estimation of $TSMc$ up to 0.500 $g\ l^{-1}$. The empirical relationship obtained confirmed the results obtained by Doxaran *et al.* (2002) using a reflectance model adapted to the Gironde estuary: the use of reflectance ratios between near-infrared and visible wavelengths reduces and even partly eliminates the effects of sediment type (grain-size, refractive index) variations occurring during regular field reflectance measurements.

To determine the limits of the established relationship, it will be applied to other measurements for the Gironde estuary and for other sites. Results should permit the development of original inversion algorithms based on reflectance ratios for SPOT, Landsat and Indian Remote Sensing satellite (IRS) sensors, in sediment-dominated coastal waters.

Acknowledgments

This work was supported by the UMR 13 (IFREMER/Université Bordeaux 1) and by PNEC-Atlantique, an oceanographic coastal French programme.

References

- AUSTIN, R. W., 1974, Inherent spectral radiance signatures of the ocean surface. In *Ocean color analysis*. Ref. 74-10, Scripps Institution of Oceanography, La Jolla, CA, USA.
- BOWERS, D. G., BOUDJELAS, S., and HARKER, G. E. L., 1998, The distribution of fine sediments in the surface waters of the Irish Sea and its relation to tidal stirring. *International Journal of Remote Sensing*, **19**, 2789–2805.
- DILLIGEAUD, E., 1997, Télédétection des eaux du cas II; caractérisations des sédiments marins. PhD thesis, University of Littoral, Côte d'Opale.
- DOXARAN, D., FROIDEFOND, J. M., LAVENDER, S. J., and CASTAING, P., 2002, Spectral signature of highly turbid waters. Application with SPOT data to quantify suspended particulate matter concentrations. *Remote Sensing of Environment*, **81**, 149–161.
- FROIDEFOND, J. M., CASTAING, P., and PRUD'HOMME, R., 1999, Monitoring suspended particulate matter fluxes and patterns with the AVHRR/NOAA-11 satellite: application to the Bay of Biscay. *Deep Sea Research II*, **46**, 2029–2055.
- GORDON, H. R., BROWN, O. B., and JACOBS, M. M., 1975, Computed relations between the inherent and apparent optical properties of a flat homogeneous ocean. *Applied Optics*, **14**, 417–427.
- LAHET, F., 1999, Caractérisation optique d'eaux côtières méditerranéennes: mesure, modélisation et inversion des réflectances. Application aux observations satellitaires. PhD thesis, University of Toulon, France.
- MOBLEY, C. D., 1994, *Light and Water: Radiative Transfer in Natural Waters* (San Diego, CA, USA: Academic Press).
- MOBLEY, C. D., 1999, Estimation of the remote-sensing reflectance from above-surface measurements. *Applied Optics*, **38**, 7442–7455.
- MOORE, G. F., AIKEN, J. and LAVENDER, S. J., 1999, The atmospheric correction of water colour and the quantitative retrieval of suspended particulate matter in case II waters: application to MERIS. *International Journal of Remote Sensing*, **20**, 1713–1733.
- MOREL, A., and GENTILI, B., 1993, Diffuse reflectance of oceanic waters. II. Bidirectional aspects. *Applied Optics*, **32**, 6864–6879.
- MOREL, A., and GENTILI, B., 1996, Diffuse reflectance of oceanic waters. III. Implication of bidirectionality for the remote-sensing problem. *Applied Optics*, **35**, 4850–4861.
- ROBINSON, M. C., MORRIS, K. P., and DYER, K. R., 1998, Deriving fluxes of suspended particulate matter in the Humber estuary, UK, using airborne remote sensing. *Marine Pollution Bulletin*, **37**, 155–163.
- SIEGLE, H., GERTH, M., and MUTZKE, A., 1999, Dynamics of the Oder river plume in the southern Baltic Sea: satellite data and numerical modelling. *Continental Shelf Research*, **19**, 1143–1159.